

Potable water hydrogenotrophic denitrification in packed-bed bioreactors coupled with a solar-electrolysis hydrogen production system

K.A. Karanasios^a, M.K. Michailides^a, I.A. Vasiliadou^a, S. Pavlou^{b,c}, D.V. Vayenas^{a,c*}

^aDepartment of Environmental and Natural Resources Management, University of Ioannina, G. Seferi 2, 30100 Agrinio, Greece
Tel. +30 26410 74117; Fax +30 26410 74176; email: dvayenas@cc.uoi.gr

^bDepartment of Chemical Engineering, University of Patras, 26504 Patras, Greece

^cInstitute of Chemical Engineering and High Temperature Chemical Processes, 26504 Patras, Greece

Received 16 January 2010; Accepted in revised form 1 October 2010

ABSTRACT

The aim of this study was to investigate the performance of bench-scale packed-bed reactors for hydrogenotrophic denitrification with hydrogen produced from electrolysis of water and electric energy provided by a solar cell. Two configurations were used, a single filter and a triple-column reactor, with gravel of different sizes as support media. The effect of hydrogen and carbon dioxide supply on the performance of the two systems of bioreactors under continuous operation was examined. The multi-filter system achieved high performances as it could safely treat polluted water with a low hydrogen and carbon dioxide consumption. A denitrification rate of 2 kg/m³d was achieved for nitrate nitrogen and hydraulic loading of 1.44 g NO₃⁻-N/d and 11.5 m³/m²d, respectively. Also, a mathematical model was developed by using growth kinetics expressions for four-nutrient limitation (nitrate, nitrite, hydrogen and carbon dioxide) with inhibition by nitrate. The proposed model is capable of describing accurately enough, hydrogenotrophic denitrification under continuous operation.

Keywords: Denitrification; Packed-bed reactors; Hydrogen production; Electrolysis; Modeling

1. Introduction

Nitrate contamination of groundwater and surface water, due to unbounded use of fertilizers and pesticides, has become a common environmental problem in many parts of the world. Nitrate- and nitrite-nitrogen removal is an important issue, since they are dangerous for public health when present in drinking water at levels above 11.3 mg NO₃⁻-N/L and 0.03 mg NO₂⁻-N/L [1]. Nitrate nitrogen (NO₃⁻-N) enrichment of receiving waters should be avoided, since drinking water containing high NO₃⁻-N concentrations is reported to increase the probability of

methemoglobinaemia (also called a blue-baby disease) and gastric cancers [2].

Biological denitrification is the process that reduces nitrate (NO₃⁻) to nitrite (NO₂⁻), to nitric oxide (NO), to nitrous oxide (N₂O), and finally to nitrogen gas (N₂). The use of autotrophic over heterotrophic denitrification ensures low biomass build-up, reduction of reactor clogging and avoidance of organic carbon contamination of treated water. Hydrogen gas (H₂) as an electron donor is an excellent autotrophic choice, due to its clean nature. It does not persist in the treated water and no further steps are required to remove either excess substrate or its derivatives [3].

* Corresponding author.

The main limitation of hydrogen-driven denitrification is the low solubility of hydrogen gas resulting in low-mass transfer rate and possible accumulation of hydrogen gas in a closed head space, thus creating an explosive environment [4]. To date, a variety of reactor configurations have been used for efficient hydrogen delivery. Many researchers have demonstrated effective hydrogenotrophic denitrification with gas permeable hollow fiber membranes, which were used to enhance the efficiency of hydrogen delivery and limit explosion risks through the bubble-less introduction of hydrogen [5,6]. The investigators focus their attention on gas-permeable membranes because they can act as both the hydrogen diffuser and the biofilm carrier. Hollow-fiber membranes are typically employed as gas-permeable membranes [7,8], although silicon tubes have been tested as well [9,10]. Hydrogen flows through the lumen and diffuses into the bulk liquid through membrane walls. Membranes offer high specific surface area and nitrate removal efficiencies, but they have high cost. The main drawback of this technology is that the precipitation of mineral solids during the denitrification process might have long-term negative impacts in a hollow fiber membrane bioreactor, which increases the operating cost [11].

Another concern regarding the use of hydrogenotrophic denitrification is the high cost of the hydrogen supplies needed, which limit its applicability. Bio-electrochemical reactor (BER) in which denitrification is stimulated with the passing of electric current might be a solution to this problem. Biofilm electrode reactors consist of a couple of electrodes [12], in which denitrifying bacteria are cultured on the cathode surface. In a BER, hydrogen gas is produced by electrolysis of water. The advantage of this process is the easy operation and maintenance; however, the denitrification rate is slow. Thus, longer hydraulic retention time is needed to achieve complete denitrification [13–16]. Moreover, excess biomass leaves the process, which calls for additional treatment.

The slow growth of the autotrophic denitrifying bacteria and the loss of biomass in the effluent, have an impact on the process efficiency. Due to the low biomass yield of hydrogenotrophic denitrifiers, most of the research conducted on hydrogenotrophic denitrification has been with attached growth systems. Nevertheless, there are limitations to the use of attached growth systems because of difficulty in biofilm control, limited mass transfer and decreasing biomass activity due to thick biofilm formation [7].

As a result, the capital and operating cost, as well as the effective denitrification of a hydrogenotrophic bioreactor must always be considered for potable water denitrification. A cheap and effective installation using silicic gravel as support media was proposed by Vasiladou et al. [17]. The size of the support media was found to affect drastically denitrification efficiency. Using a

triple-column reactor, high nitrate concentrations up to 340 mg NO_3^- -N/L were treated.

Most of the studies reported in the literature used commercially available hydrogen, which raise the operating cost of clean potable water production. On the other hand some efforts have been conducted for cheap hydrogen production. Grommen et al. [18] and Lu et al [19] generated hydrogen gas with electrolytic cells. Vagheei et al. [20] produced in situ hydrogen and carbon dioxide by the electrolysis of methanol. Finally, a multi-electrode system for BER reactors was proposed from Sakakibara and Nakayama [21] and Prosnansky et al [22] for hydrogen production, where in the later case the operating cost was about 0.18–0.67 US\$/m³ of treated water.

The aim of the present work was to investigate the hydrogenotrophic denitrification activity by in situ hydrogen production in order to reduce operating cost. Hydrogen was produced on-line at atmospheric pressure, through a system of electrolysis with energy supplied from a solar cell. Experiments were conducted by using two different bioreactor configurations, in order to investigate the effect of supplied quantities of hydrogen and carbon dioxide on the reactors' performance under continuous operating mode. Finally, a mathematical model able to predict nitrate and nitrite utilization, as well as H₂ and CO₂ consumption during denitrification process under various operating conditions was developed.

This is the first time that the electric energy which is required by the electrolysis cell is generated from the solar energy, thus reducing practically to zero the operating cost of a treatment plant. In addition, the use of inexpensive support media can make the hydrogenotrophic denitrification economically viable for potable water treatment.

2. Materials and methods

2.1. Enrichment culture

The mixed culture utilized in the present work had been acclimatized in a former study [23]. The hydrogen-oxidizing denitrification culture was enriched from activated sludge taken from the wastewater treatment plant of the city of Agrinio, Greece. Seed sludge was added to a 2 L flask containing nitrate (KNO₃ 0.722 g/L), tap water, and buffer (KH₂PO₄ 3.39 g/L and Na₂HPO₄ 3.53 g/L). Anoxic conditions were used to enrich the culture, while it was continuously sparged with a gas mixture comprising CO₂ and H₂.

2.2. Experimental system

Three packed-bed reactors were used for the experiments. The packed-bed reactors consisted of a Plexiglas tube, 52 cm high and 4 cm i.d. The overall volume of each reactor was 650 ml. The working volume of the filters was

250 ml. The support material was gravel with a depth of 40 cm. The mean diameters of the support media were 1.75 mm, 2.41 mm and 4.03 mm. The porosity of these media was 0.39, 0.4 and 0.42, respectively, while the specific surface areas were 32.07, 22.74 and 14.16 cm²/cm³, respectively. Experiments were performed by using two bioreactor systems: the first system (system I) was a filter with gravel of 2.41 mm mean diameter and the second system (system II) consisted of three filters in series with three different gravel sizes (1st filter with gravel of 4.03 mm mean diameter, 2nd 2.41 mm and 3rd 1.75 mm). A detailed description of the experimental set-up has been given by Vasiliadou et al. [17].

Throughout the experiments, carbon dioxide and hydrogen were sparged from the bottom of the filters. Along the depth of filters there were four sampling ports for nitrate, nitrite, and CO₂ and H₂ concentration measurements in the bulk liquid. Hydrogen is used by the hydrogen oxidizing bacteria as electron donor, while carbon dioxide is used as the carbon source for biosynthesis. In addition, CO₂ was used for pH adjustment in order to avoid pH rise, since phosphate buffers were not used in the system [24]. The feed solution (synthetically produced contaminated water) was composed of tap water and KNO₃ (0.72 g/L → 100 mg NO₃⁻-N/L) as the contaminant. Throughout the reactors' operation the systems were maintained at a temperature of 26±1°C, while the pH was maintained at 6.8±0.2.

2.3. Analytical methods

Concentration measurements of nitrate and nitrite nitrogen were performed on a daily basis during all experiments. The liquid samples were centrifuged for 5 min at 14000 rpm (Eppendorf Centrifuge 5424) to remove any suspended solids and the supernatants were then analyzed. Each experiment was performed three times to ensure reproducibility. Nitrate and nitrite concentrations were measured according to the Standard Methods for the Examination of Water and Wastewater [25] by using a UV/Vis spectrophotometer (Boeco S-22 UV/VIS) and following the procedure of the 4500-NO₃⁻-B and the colorimetric of 4500-NO₂⁻-B method, respectively. The pH was measured with Consort C835 a multi-parameter analyzer [25]. Dissolved H₂ and CO₂ concentrations were measured by the headspace-GC method [26] using a gas chromatography (GC, SRI 8610C) equipped with HID detector.

2.4. Hydrogen production

The hydrogen used in all experiments was produced in the laboratory by electrolysis of water. The electric energy supplied to the Proton Exchange Membrane (PEM) Electrolyzer came from a solar cell. This system of hydrogen production solves the problem of high cost of hydrogen supply during implementation at a

Table 1

Special features of the solar-electrolysis hydrogen production system

PEM electrolyzer – solar cell	
Feature	Value
Hydrogen production, L/h	14.5
Maximum pressure	Atmospheric
Hydrogen, %	>99.9
Water consumption, L/h	0.1
Water	Distilled
Power/voltage/current	50 W/14 V dc/4 A
Dimensions (L × W × H), mm	190–264–200
Number of cells	7
Electrode area, cm ²	16
Electrode material	Carbon
Electrode enrichment	Platinum
Area of solar cell, m ²	2.40

drinking-water treatment plant. The features of the solar-electrolyzer system are shown in Table 1.

3. Results and discussion

3.1. Bioreactor acclimation

After cultivation of microorganisms, the hydrogenotrophic culture was transferred to the bioreactors. During a 2-month start-up period, filters were operated as batch systems (data not shown) to ensure attachment of the bacterial culture on the support media and development of a biofilm layer. As soon as nitrate degradation was completed, 50 ml of fresh contaminated water, which contained tap water, KNO₃ (2.88 g/L), KH₂PO₄ (3.39 g/L), Na₂HPO₄ (3.53 g/L), was added to the reactors, to bring nitrate concentration to its initial level (80 mg NO₃⁻-N/L). This operating cycle was repeated systematically until its duration reduced to only a couple of hours. After about two months, a uniform biofilm was visible on the surface of gravels. At that time it was decided to switch to continuous operation.

3.2. Continuous operation

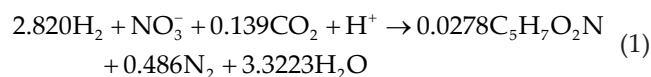
3.2.1. Continuous operation – single filter

The filter with gravel of 2.41 mm mean diameter (system I) was used to investigate the performance of hydrogenotrophic denitrification under continuous mode. The filter was kept in continuous operation for more than 4 months, before the experimental series took place, in order to ensure that pseudo steady state of the biofilm would be achieved. During continuous operation, water with upflow volumetric rate (VFR) of 5 ml/

min (hydraulic loading $5.7 \text{ m}^3/\text{m}^2\text{d}$) was added with feed concentration $100 \text{ mg NO}_3^-/\text{L}$. The nitrate nitrogen loading in the system was $0.72 \text{ g NO}_3^-/\text{d}$. During the experiments of continuous operation, the addition of phosphoric buffers, which were used in the acclimation of the hydrogenotrophic culture and of the bioreactors' biofilm to enhance biomass growth, was interrupted. The pH was maintained at 6.8 ± 0.2 with adjustment by CO_2 supplied to the system.

Filter washing was necessary to avoid operating problems due to pore clogging from biomass growth and for better circulation of the gases (H_2 , CO_2) in the reactor. Washing was performed once every six days with 2 L of water, using high water ($4 \text{ L}/\text{min}$) upflow velocity and gases (with a flow rate of $300 \text{ ml}/\text{min}$) periodically. Before sampling, the filter was washed and then operated in continuous mode, while keeping the influent conditions constant for at least 3 d in order to ensure pseudo-steady-state conditions. The sampling was being done from the third to the fifth day, for each set of operating conditions. Sampling was performed at each sampling valve with an immersed syringe reaching the centre of the filter. Each point in the plots is the result of three measurements.

In order to estimate the optimum hydrogen and carbon dioxide dose, a theoretical approach was necessary. The overall reaction of autohydrogenotrophic denitrification [Eq. (1)] reveals that 2.82 mol of H_2 and 0.139 mol of CO_2 (in the form of carbon dioxide gas) are required to reduce 1 mol of nitrate (NO_3^-) to inert nitrogen gas [24,27].



Namely, the process requires 0.403 mg H_2 and 0.437 mg CO_2 per $\text{mg NO}_3^-/\text{N}$. In a previous work, Vasiliadou and co-workers [17] reported that for the same nitrogen loading, $30 \text{ ml}/\text{min}$ carbon dioxide and

$90 \text{ ml}/\text{min}$ hydrogen were supplied to the reactor provided a hydrogen and carbon dioxide over nitrogen mass ratio of 16.18 mg H_2 and 118.62 mg CO_2 per $\text{mg NO}_3^-/\text{N}$. These ratios were chosen to be that high to ensure that gases were not rate-limiting. However, experiments in system I were designed for optimization of gas doses, concerning low cost and high denitrification efficiency. Thus, the first attempt was carried out with H_2 and CO_2 supplied to the system with flow rates of 24.4 and $4.7 \text{ ml}/\text{min}$, respectively, in order to achieve a good performance with a lower gas sparging. The mass ratios of the supplied hydrogen and carbon dioxide over nitrogen were 4.386 mg H_2 and 18.6 mg CO_2 per $\text{mg NO}_3^-/\text{N}$, respectively (Table 2). These mass ratios were lower than those previously reported [17], however higher doses of carbon and electron donor than the theoretical demand were applied to provide abundance of supply and prevent any possible deficiency. It must be noted that the hydrogen over carbon gas ratio that was used in the system was $\text{H}_2/\text{CO}_2 = 5/1$, according to the flow rate ratios ($\text{ml H}_2/\text{ml CO}_2$) supplied to other hydrogenotrophic systems [20,28]. Also, since hydrogen was provided by the solar-electrolysis hydrogen production system without any cost, the only operating cost of the process concerned carbon dioxide.

Fig. 1 presents the experimentally measured NO_3^-/N , NO_2^-/N (Fig. 1a), H_2 and CO_2 (Fig. 1b) concentrations along the filter (system I) for the first combination of gas concentrations. The horizontal solid and dash lines represent the highest permitted nitrate- and nitrite-nitrogen concentration limits of 11.3 and $0.03 \text{ mg}/\text{L}$, respectively. As shown in Fig. 1a, safe removal of nitrates from water was observed, since at the effluent, the NO_3^-/N and NO_2^-/N concentrations were below the permitted limits (Table 2). The dissolved H_2 concentration ranged between 0.82 and $1.25 \text{ mgH}_2/\text{L}$ (Fig. 1b), decreasing gradually from the influent to the middle stage of the reactor, where elimination of a great quantity of NO_3^-/N took place. The

Table 2
Operating conditions of the two bioreactors

Description	Single filter				Multi filter					
	Run 1		Run 2		Run 3		Run 4		Run 5	
	H_2	CO_2	H_2	CO_2	H_2	CO_2	H_2	CO_2	H_2	CO_2
Gas flow rate, ml/min	24.4	4.7	20.0	3.3	10.0	1.5	4.6	0.8	3.0	0.8
Gas ratio, $\text{mgH}_2/\text{mgCO}_2$	1/4.240		1/3.633		1/3.303		1/3.831		1/5.874	
Experimental ratio, $\text{mg gas}/\text{mg NO}_3^-/\text{N}$	4.386	18.6	3.595	13.060	0.899	2.97	0.413	1.584	0.269	1.584
Theoretical ratio, $\text{mg gas}/\text{mgNO}_3^-/\text{N}$	0.403	0.437	0.403	0.437	0.403	0.437	0.403	0.437	0.403	0.437
Water flow rate, ml/min	5				10					
Influent NO_3^-/N , mg/L	100				100					
Effluent NO_3^-/N , mg/L	8.04		11.83		2.06		2.76		2.31	
Effluent NO_2^-/N , mg/L	0		0.033		0		0		0	

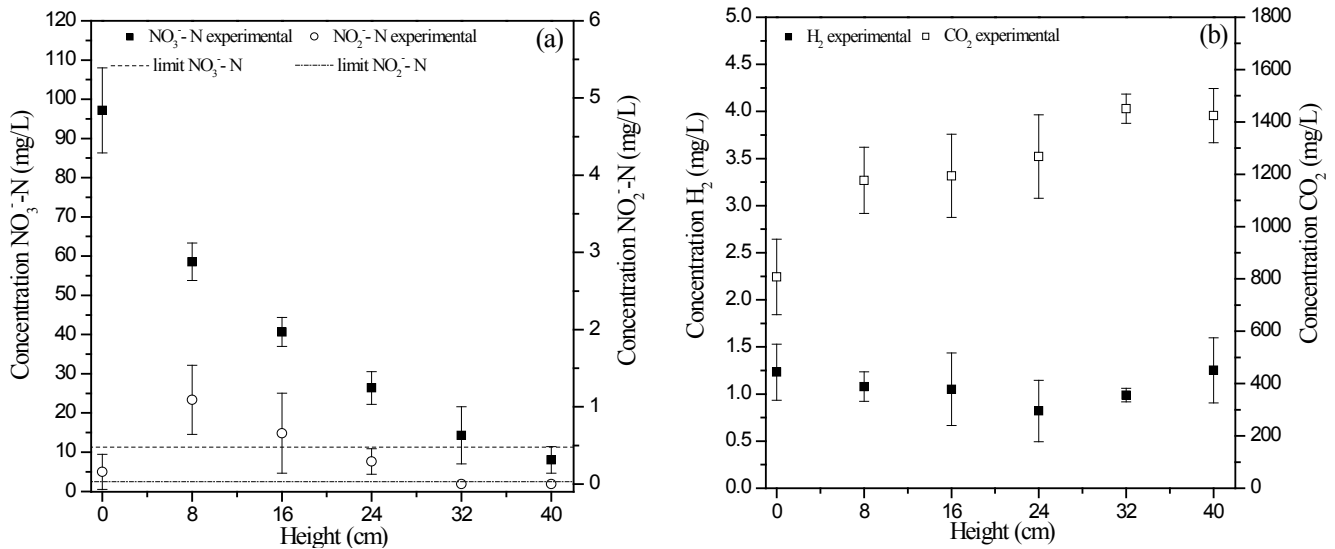


Fig. 1. Continuous operation of bioreactor with gravel of 2.41 mm diameter. Experimentally determined (a) NO_3^- -N and NO_2^- -N and (b) H_2 and CO_2 concentrations along the filter height for H_2 and CO_2 flow rates of 24.4 and 4.7 ml/min, respectively.

dissolved CO_2 concentration ranged between 0.98 and 1.45 g CO_2 /L (Fig. 1b) with gradually increase from the influent to the effluent of the reactor, as the consumption was low compared to the dissolution of the CO_2 .

In an effort to reduce the gases waste and as a result the operating cost of the operation of system I, the flow rates of H_2 and CO_2 were further reduced to 20.0 and 3.3 ml/min, respectively. The ratios of the supplied H_2 and CO_2 quantities over nitrogen mass are shown in Table 2. It was observed that, for lower gas flow rates, lower con-

centrations of carbon dioxide were realized in the system (Fig. 2b), while hydrogen concentrations were at the same level as in the first experiment.

As shown in Fig. 2a, although safe removal of nitrate- and nitrite- nitrogen was observed, the system reached its operational critical upper limits. In order to decrease even further the operation cost and increase the bioreactor's performance, an extension of the system's length, which would lead to greater dissolution of the gases, was considered to be necessary.

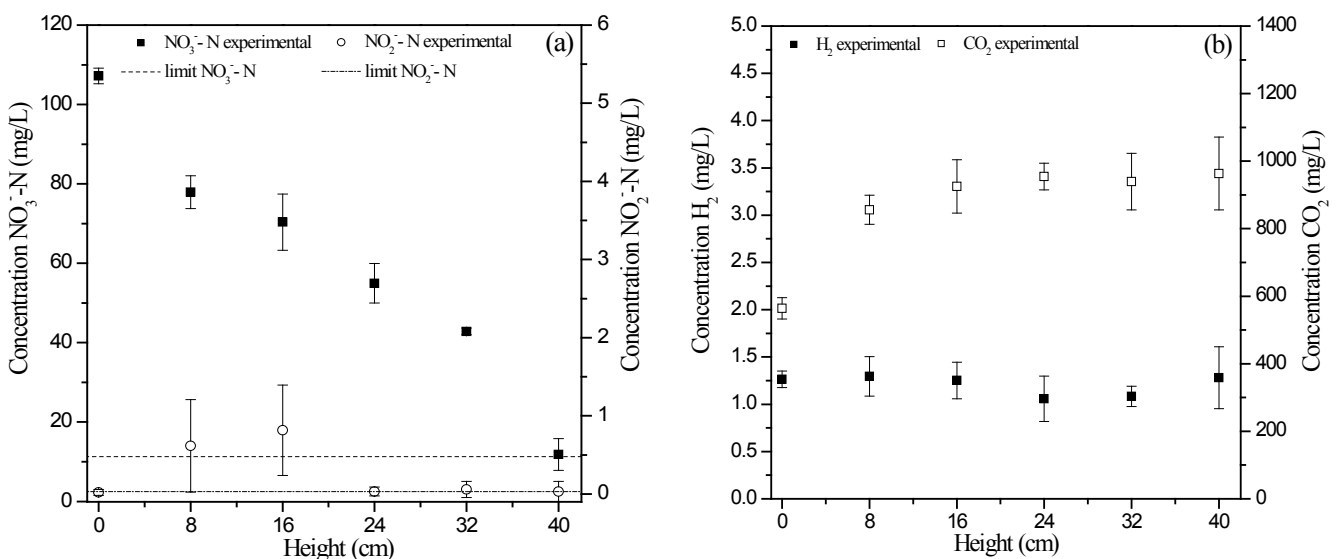


Fig. 2. Continuous operation of bioreactor with gravel of 2.41 mm diameter. Experimentally determined (a) NO_3^- -N and NO_2^- -N and (b) H_2 and CO_2 concentrations along the filter height for H_2 and CO_2 flow rates of 20.0 and 3.3 ml/min, respectively.

3.3.2. Continuous operation – multi-filter

In order to increase the bioreactor performance a triple-column bioreactor was set up. The effect of the supplied quantities of hydrogen and carbon dioxide on the performance of three filters (system II) in series with three different gravel sizes (4.03, 2.41 and 1.75 mm mean diameters), was investigated. The three filters in series increase the length of the system and, as a result, the retention time of water and gases in the reactor. The first filter was chosen to be the one with the gravel of 4.03 mm in order to avoid pore clogging due to the high loadings. The filter with gravel of 1.75 mm was decided to be the last one to receive lower loadings in order to avoid any operating problems. During continuous operation, water with upflow volumetric rate of 10 ml/min and hydraulic loading of $11.5 \text{ m}^3/\text{m}^2\text{d}$ was added with feed concentration $100 \text{ mg NO}_3^-/\text{L}$. The nitrate nitrogen loading to system II was $1.44 \text{ g NO}_3^-/\text{d}$.

The filters were kept at continuous operation for more than 4 months, before the experimental series took place, in order to ensure that pseudo steady state would be achieved. Sampling and filter backwash were carried out following the same procedure described above. Each value in the plots is the result of three measurements.

Initially, H_2 and CO_2 were fed to the system II with flow rates of 10.0 and 1.5 ml/min, respectively. It was observed that, as the nitrate nitrogen loading was doubled, the flow rates of the gases were much lower than those supplied to the system I. The H_2 and CO_2 supplied to the system gave hydrogen and carbon dioxide over nitrogen mass ratio of 0.899 mg H_2 and $2.970 \text{ mg CO}_2 / \text{mg NO}_3^-/\text{N}$, respectively (Table 2). Fig. 3 shows the experimentally determined nutrient concentrations along the triple-

column bioreactor. As shown in Table 2, safe removal of nitrates from water was observed, since at the effluent the NO_3^-/N and NO_2^-/N concentrations were 2.06 and 0.0 mg/L , respectively.

Two additional experiments (Figs. 4 and 5) were conducted in an attempt to further decrease the carbon dioxide and hydrogen doses. Fig. 4 depicts the second experimental trial, with H_2 and CO_2 supplied to the system at flow rates of 4.6 and 0.8 ml/min, respectively. The H_2 and CO_2 provide an experimental ratio ($\text{mg gas}/\text{mg NO}_3^-/\text{N}$) still higher than the theoretical (Table 2). Consumption of these two nutrients was further reduced, while maintaining safe treatment of the polluted water. Finally, the last experiment (Fig. 5) was carried out with hydrogen flow rate of 3.0 ml/min, while the carbon dioxide was maintained at the value of 0.8 ml/min. A further decrease of CO_2 caused nitrite nitrogen accumulation and a pH rise to 9 (data not shown). Although, the H_2 supplied had a ratio ($\text{mg gas}/\text{mg NO}_3^-/\text{N}$) lower of than the theoretically required, safe removal of nitrates and nitrites from water was achieved (Fig. 5a). The proposed system seems to be very effective for potable water denitrification, as all the three runs which were conducted, achieved high performance with a denitrification rate of 2 g/Ld .

4. Mathematical modelling

As mentioned above, the three-column filter was the optimum as far as efficiency and operating cost are concerned. Thus, a model of this system was used to simulate the process of hydrogenotrophic denitrification for various operating conditions. We adopted the mathematical model that has been described by Vasiliadou

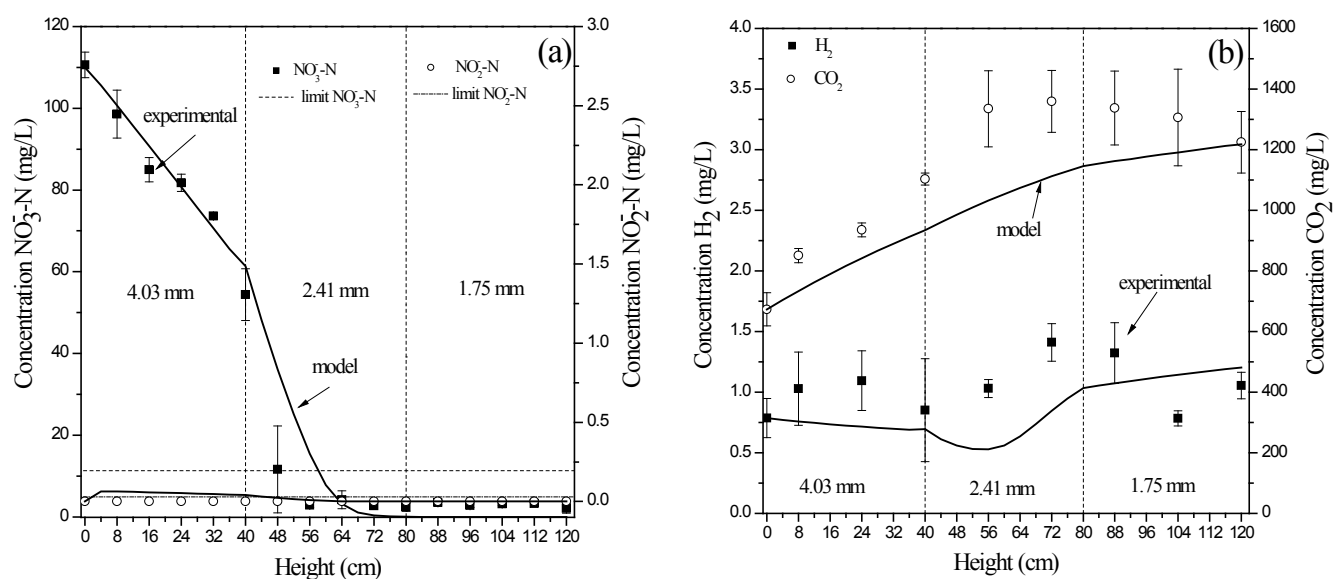


Fig. 3. Continuous operation of the three-filter system. Experimentally determined (a) NO_3^-/N and NO_2^-/N and (b) H_2 and CO_2 concentrations along the filter height and the corresponding model predictions, for gas flow rates of 10.0 and 1.5 ml/min.

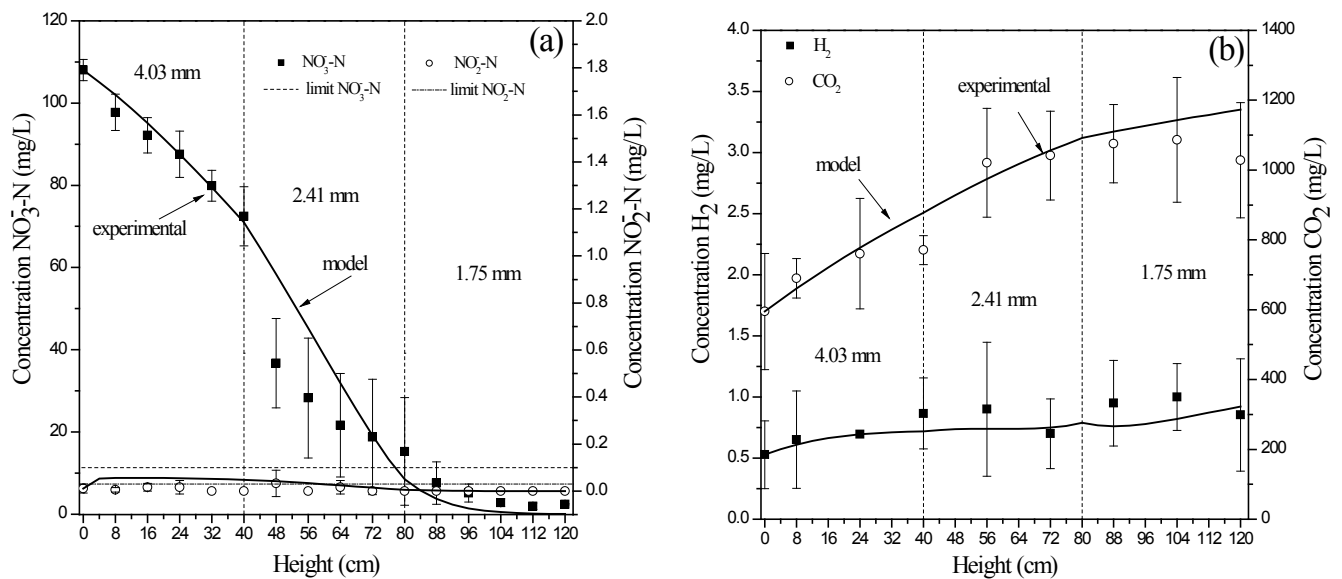


Fig. 4. Continuous operation of the three-filter system. Experimentally determined (a) NO_3^- -N and NO_2^- -N and (b) H_2 and CO_2 concentrations along the filter height and the corresponding model predictions, for gas flow rates of 4.6 and 0.8 ml/min.

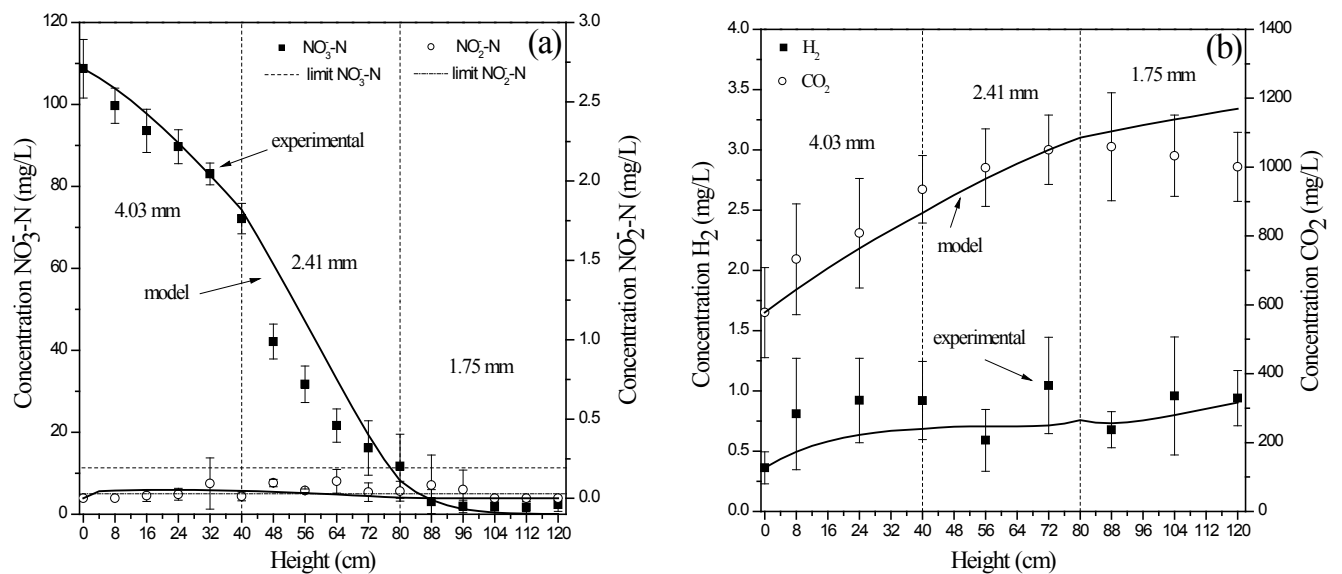


Fig. 5. Continuous operation of the three-filter system. Experimentally determined (a) NO_3^- -N and NO_2^- -N and (b) H_2 and CO_2 concentrations along the filter height and the corresponding model predictions, for gas flow rates of 3.0 and 0.8 ml/min.

et al. [17]. However, in the present study, the kinetics of growth of hydrogen oxidation bacteria was assumed to be subject to four-nutrient limitation (with nitrate, nitrite, carbon dioxide and hydrogen as the primary nutrients of interest) with inhibition by nitrate. Nitrate and nitrite are considered as nutrients which fulfil the need of the micro-organisms for electron acceptors. The nitrate elimination

was modelled using an Andrews-type expression [29] for nitrate inhibition, while nitrite reduction was modelled by a Monod expression. Hydrogen and carbon dioxide were considered as supplementary nutrients together with nitrate or nitrite, while their limitations were modelled by Monod expressions. The kinetic expressions are given by the following equations:

$$\mu(C_{\text{NO}_3\text{NI}}) = \frac{r_{\text{max}1} C_{\text{NO}_3\text{NI}}}{K_s + C_{\text{NO}_3\text{NI}} + k_{d2} C_{\text{NO}_2\text{NI}} + \frac{C_{\text{NO}_3\text{NI}}^2}{K_i}} \cdot \frac{C_{\text{H}_2\text{NI}}}{K_{\text{SH}_2} + C_{\text{H}_2\text{NI}}} \cdot \frac{C_{\text{CO}_2\text{NI}}}{K_{\text{SCO}_2} + C_{\text{CO}_2\text{NI}}} \quad (2)$$

$$\mu(C_{\text{NO}_2\text{NI}}) = \frac{r_{\text{max}2} C_{\text{NO}_2\text{NI}}}{K_n + C_{\text{NO}_2\text{NI}} + k_{d1} C_{\text{NO}_3\text{NI}}} \cdot \frac{C_{\text{H}_2\text{NI}}}{K_{\text{NH}_2} + C_{\text{H}_2\text{NI}}} \cdot \frac{C_{\text{CO}_2\text{NI}}}{K_{\text{NCO}_2} + C_{\text{CO}_2\text{NI}}} \quad (3)$$

where $C_{\text{NO}_3\text{NI}}$ and $C_{\text{NO}_2\text{NI}}$ are the nitrate and nitrite nitrogen concentration (mg/cm^3), respectively, $C_{\text{H}_2\text{NI}}$ and $C_{\text{CO}_2\text{NI}}$ are the dissolved hydrogen and carbon dioxide concentration (mg/cm^3), respectively, at every NI compartment of the bioreactor, $r_{\text{max}1}$ and $r_{\text{max}2}$ (1/h) are the maximum specific growth rates of nitrate and nitrite, respectively, K_s and K_n (mg/cm^3) are the saturation constant for nitrate and nitrite, respectively, K_{SH_2} and K_{NH_2} (mg/cm^3) are the saturation constants for H_2 , K_{SCO_2} and K_{NCO_2} (mg/cm^3) are the saturation constants for CO_2 , K_i (mg/cm^3) is the nitrate inhibition constant, k_{d1} ($\text{mg NO}_2^-/\text{N}/\text{mg NO}_3^-/\text{N}$) and k_{d2} ($\text{mg NO}_3^-/\text{N}/\text{mg NO}_2^-/\text{N}$) are constants in the growth rate expressions.

In order to describe the continuous operation, the assumptions used by Vasiliadou et al. [17] were adopted.

Mass balances for nitrate, nitrite, carbon dioxide and hydrogen inside the biofilm in the NI compartment of the filter yield the following equations:

$$-D_{\text{NO}_3} \phi \frac{\partial^2 C_{\text{NO}_3\text{NI}}}{\partial z^2} + \phi \frac{\partial C_{\text{NO}_3\text{NI}}}{\partial t} + \frac{1}{Y_s} \mu(C_{\text{NO}_3\text{NI}}) X = 0 \quad (4)$$

$$-D_{\text{NO}_2} \phi \frac{\partial^2 C_{\text{NO}_2\text{NI}}}{\partial z^2} + \phi \frac{\partial C_{\text{NO}_2\text{NI}}}{\partial t} + \frac{1}{Y_n} \mu(C_{\text{NO}_2\text{NI}}) X - \frac{1}{Y_s} \mu(C_{\text{NO}_3\text{NI}}) X = 0 \quad (5)$$

$$-D_{\text{CO}_2} \phi \frac{\partial^2 C_{\text{CO}_2\text{NI}}}{\partial z^2} + \phi \frac{\partial C_{\text{CO}_2\text{NI}}}{\partial t} + \frac{1}{Y_{\text{NCO}_2}} \mu(C_{\text{NO}_2\text{NI}}) X + \frac{1}{Y_{\text{SCO}_2}} \mu(C_{\text{NO}_3\text{NI}}) X = 0 \quad (6)$$

$$-D_{\text{H}_2} \phi \frac{\partial^2 C_{\text{H}_2\text{NI}}}{\partial z^2} + \phi \frac{\partial C_{\text{H}_2\text{NI}}}{\partial t} + \frac{1}{Y_{\text{NH}_2}} \mu(C_{\text{NO}_2\text{NI}}) X + \frac{1}{Y_{\text{SH}_2}} \mu(C_{\text{NO}_3\text{NI}}) X = 0 \quad (7)$$

where X is the biomass density (mg/cm^3), D is the diffusion coefficient (cm^2/h), Y_x $\text{mg biomass}/\text{mg } x$ is the growth yield coefficient on the x substrate and ϕ is the biofilm porosity. Eqs. (4)–(7) result by considering the processes of nitrate, nitrite, H_2 and CO_2 diffusion and consumption and/or generation inside the biofilm in the NI compartment of the filter.

Mass balances for nitrate, nitrite, carbon dioxide and hydrogen in the bulk liquid in the NI compartment of the filter yield the following equations:

$$\varepsilon \frac{dC_{\text{NO}_3\text{BNI}}}{dt} = \frac{Q}{V_{\text{NI}}} (C_{\text{NO}_3\text{BNI-1}} - C_{\text{NO}_3\text{BNI}}) - A_s (1 - \varepsilon) D_{\text{NO}_3} \phi \frac{\partial C_{\text{NO}_3\text{NI}}}{\partial z} \Big|_{z=L} - A_s (1 - \varepsilon) u_L \phi C_{\text{NO}_3\text{NI}} \quad (8)$$

$$\varepsilon \frac{dC_{\text{NO}_2\text{BNI}}}{dt} = \frac{Q}{V_{\text{NI}}} (C_{\text{NO}_2\text{BNI-1}} - C_{\text{NO}_2\text{BNI}}) - A_s (1 - \varepsilon) D_{\text{NO}_2} \phi \frac{\partial C_{\text{NO}_2\text{NI}}}{\partial z} \Big|_{z=L} - A_s (1 - \varepsilon) u_L \phi C_{\text{NO}_2\text{NI}} \quad (9)$$

$$\varepsilon \frac{dC_{\text{CO}_2\text{BNI}}}{dt} = \frac{Q}{V_{\text{NI}}} (C_{\text{CO}_2\text{BNI-1}} - C_{\text{CO}_2\text{BNI}}) + K_{\text{LCO}_2} a_{\text{CO}_2} (C_{\text{CO}_2}^* - C_{\text{CO}_2\text{BNI}}) - A_s (1 - \varepsilon) D_{\text{CO}_2} \phi \frac{\partial C_{\text{CO}_2\text{NI}}}{\partial z} \Big|_{z=L} - A_s (1 - \varepsilon) u_L \phi C_{\text{CO}_2\text{NI}} \quad (10)$$

$$\varepsilon \frac{dC_{\text{H}_2\text{BNI}}}{dt} = \frac{Q}{V_{\text{NI}}} (C_{\text{H}_2\text{BNI-1}} - C_{\text{H}_2\text{BNI}}) + K_{\text{LH}_2} a_{\text{H}_2} (C_{\text{H}_2}^* - C_{\text{H}_2\text{BNI}}) - A_s (1 - \varepsilon) D_{\text{H}_2} \phi \frac{\partial C_{\text{H}_2\text{NI}}}{\partial z} \Big|_{z=L} - A_s (1 - \varepsilon) u_L \phi C_{\text{H}_2\text{NI}} \quad (11)$$

where Q is the volumetric flow rate (cm^3/h) and V_{NI} is the volume of each compartment (cm^3), A_s (cm^2/cm^3) is the support media specific surface area, ε is the reactor porosity, L (cm) is the biofilm thickness, u_L (cm/h) is the velocity of the biofilm surface, K_{LH_2} and K_{LCO_2} are the mass transfer coefficients (cm/h) for the gases and a_{H_2} and a_{CO_2} are the specific surface areas of H_2 and CO_2 gas bubble (cm^2/cm^3), respectively. $C_{\text{H}_2}^*$ and $C_{\text{CO}_2}^*$ (mg/cm^3) are the calculated dissolved H_2 and CO_2 equilibrium concentrations by Henry's law with the Henry's law constants in aqueous solutions at 26°C [30].

The first terms in the right-hand-side in Eqs. (8)–(11) represent the difference between the inlet and the outlet of nutrients in the bulk liquid in the NI compartment of the filter, while the third terms represent the nutrients' diffusion from the bulk liquid to the biofilm in the same compartment.

The mass balance equation for biomass detached from the biofilm surface area, in the bulk fluid in the NI compartment of the filter is:

$$\varepsilon \frac{dX_{\text{BNI}}}{dt} = \frac{Q}{V_{\text{NI}}} (X_{\text{BNI}-1} - X_{\text{BNI}}) + \left(\mu(C_{\text{NO}_3\text{BNI}}) X_{\text{BNI}} + \mu(C_{\text{NO}_2\text{BNI}}) X_{\text{BNI}} - k_d X_{\text{BNI}} \right) \varepsilon + A_s (1 - \varepsilon) u_{\text{det}} X \quad (12)$$

where u_{det} (cm/h) is the detachment velocity by which particulate components are detached from the biofilm surface [17] and k_d (1/h) is the death rate constant.

The nutrients consumed by detached biomass were negligible, thus it was assumed that the elimination of the nutrient in the bulk liquid was zero.

The boundary conditions for the system of equations are:

$$\text{B.C. 1: } \frac{\partial C_{\text{NO}_3\text{NI}}(0, t)}{\partial z} = 0 \quad (13)$$

$$\text{B.C. 2: } \frac{\partial C_{\text{NO}_2\text{NI}}(0, t)}{\partial z} = 0 \quad (14)$$

$$\text{B.C. 3: } \frac{\partial C_{\text{CO}_2\text{NI}}(0, t)}{\partial z} = 0 \quad (15)$$

$$\text{B.C. 4: } \frac{\partial C_{\text{H}_2\text{NI}}(0, t)}{\partial z} = 0 \quad (16)$$

$$\text{B.C. 5: } C_{\text{NO}_3\text{NI}}(L, t) = C_{\text{NO}_3\text{BNI}} \quad (17)$$

$$\text{B.C. 6: } C_{\text{NO}_2\text{NI}}(L, t) = C_{\text{NO}_2\text{BNI}} \quad (18)$$

$$\text{B.C. 7: } C_{\text{CO}_2\text{NI}}(L, t) = C_{\text{CO}_2\text{BNI}} \quad (19)$$

$$\text{B.C. 8: } C_{\text{H}_2\text{NI}}(L, t) = C_{\text{H}_2\text{BNI}} \quad (20)$$

and the initial conditions are:

$$\text{I.C.1 } C_{\text{NO}_3\text{BNI}}(0) = C_{\text{NO}_3\text{entrance}} \quad (21)$$

$$\text{I.C. 2: } C_{\text{NO}_2\text{BNI}}(0) = C_{\text{NO}_2\text{entrance}} \quad (22)$$

$$\text{I.C. 3: } C_{\text{CO}_2\text{BNI}}(0) = C_{\text{CO}_2\text{entrance}} \quad (23)$$

$$\text{I.C. 4: } C_{\text{H}_2\text{BNI}}(0) = C_{\text{H}_2\text{entrance}} \quad (24)$$

where C_{entrance} is the substrate concentration at the entrance of the filter (mg/cm^3).

$$\text{I.C. 5: } C_{\text{NO}_3\text{NI}}(z, 0) = 0 \quad (25)$$

$$\text{I.C. 6: } C_{\text{NO}_2\text{NI}}(z, 0) = 0 \quad (26)$$

$$\text{I.C. 7: } C_{\text{CO}_2\text{NI}}(z, 0) = 0 \quad (27)$$

$$\text{I.C. 8: } C_{\text{H}_2\text{NI}}(z, 0) = 0 \quad (28)$$

and

$$\text{I.C. 9: } X_{\text{BNI}}(0) = 0 \quad (29)$$

All kinetic parameters, except from diffusion coefficients [31], were evaluated from simulation of the experimental data. Data fitting (Figs. 3, 4 and 5) was performed using Aquasim (Version 2.1d) computer code. The computed values of the kinetic parameters of the model are listed in Table 3.

To simulate the continuous operation of the three filters in series (multi-stage filter) (Figs. 3–5), the reactors were modelled as a combination of thirty completely mixed biofilm compartments connected by advective links using the Aquasim program. As mentioned above, the sampling was taking place from the third to the fifth day (after washing), for each set of operating conditions. The biofilm thickness at the beginning of operation (after washing) was estimated to be different for each combination of carbon dioxide and hydrogen flow and for each reactor. These differences in the initial value of the biofilm thickness are due to the different nitrogen and gas loadings in each reactor and to the different support media in the three filters.

The Aquasim program calculates the development of the biofilm thickness and the theoretical predictions for the nitrate-, nitrite-nitrogen, CO_2 and H_2 concentrations at the third, fourth and fifth day of filter's operation. It must be noted that the experimental data used in the data fitting process of the Aquasim program, were the mean values of sampling at the third, fourth and fifth day.

Figs. 3, 4 and 5 show the profiles of nitrate-, nitrite-nitrogen, CO_2 and H_2 concentrations along system II, as obtained from the experiments and predicted by the model. The theoretical predictions (solid lines) for the nutrient concentrations shown in Figs. 3–5, are the predictions for the fourth day of operation. It can be seen that the model predictions matched well the experimental data. The only case that the model failed to predict the experimental data is the hydrogen consumption in the second filter (gravel $d = 2.41$ mm) for H_2 and CO_2 flow rates of 24.4 and 4.7 ml/min (Fig. 3b), respectively. The models failure is due to the fact that the initial value of the biofilm thickness in this filter (Table 3) is too high and results to the prediction by the model of high hydrogen elimination.

5. Conclusions

Two bench-scale bioreactor systems were tested in order to study the effect of the supplied quantities of hydrogen and carbon dioxide on the hydrogenotrophic denitrification efficiency. The main conclusions from this work are:

- A comparison between the two systems of water treatment showed that, the three-bioreactors system can treat safely twice as much nitrate nitrogen loading, with a drastic reduction of H_2 and CO_2 consumption.

Table 3
Model parameter values

Parameter	Value					
	Run 3		Run 4		Run 5	
	H ₂	CO ₂	H ₂	CO ₂	H ₂	CO ₂
Gas flow rate, ml/min	10.0	1.5	4.6	0.8	3.0	0.8
D_{NO_3} , cm ² /h				0.0683		
D_{NO_2} , cm ² /h				0.0683		
D_{CO_2} , cm ² /h				0.0691		
D_{H_2} , cm ² /h				0.2104		
$C_{\text{H}_2}^*$, mg/cm ³				1.51×10 ⁻³		
$C_{\text{CO}_2}^*$, mg/cm ³				1.488		
$K_{\text{LH}_2} a_{\text{H}_2}$ (Filter 1.75 mm), 1/h				1.201		
$K_{\text{LH}_2} a_{\text{H}_2}$ (Filter 2.41 mm), 1/h				4.545		
$K_{\text{LH}_2} a_{\text{H}_2}$ (Filter 4.03 mm), 1/h				3.021		
$K_{\text{LCO}_2} a_{\text{CO}_2}$ (Filter 1.75 mm), 1/h				0.655		
$K_{\text{LCO}_2} a_{\text{CO}_2}$ (Filter 2.41 mm), 1/h				1.205		
$K_{\text{LCO}_2} a_{\text{CO}_2}$ (Filter 4.03 mm), 1/h				1.087		
$r_{\text{max}1}$, 1/h				0.152		
K_{S} , mg/cm ³				0.0083		
K_{SH_2} , mg/cm ³				0.0253		
K_{SCO_2} , mg/cm ³				0.0285		
Y_{S} , mg biomass/mg NO ₃ ⁻ -N				0.128		
Y_{SH_2} , mg biomass/mg H ₂				6.586		
Y_{SCO_2} , mg biomass/mg CO ₂				3.346		
K_{I} , mg/cm ³				0.178		
$r_{\text{max}2}$, 1/h				0.834		
K_{N} , mg/cm ³				0.0384		
K_{NH_2} , mg/cm ³				3.65×10 ⁻⁴		
K_{NCO_2} , mg/cm ³				7.71×10 ⁻⁴		
Y_{N} , mg biomass/mg NO ₂ ⁻ -N				1.06×10 ⁻³		
Y_{NH} , mg biomass/mg H ₂				5.411		
Y_{NCO_2} , mg biomass/mg CO ₂				1.414		
k_{d} , 1/h				1.46×10 ⁻⁵		
$k_{\text{d}1}$, mg NO ₂ ⁻ -N/mg NO ₃ ⁻ -N				16.48		
$k_{\text{d}2}$, mg NO ₃ ⁻ -N/mg NO ₂ ⁻ -N				28.67		
L (Filter 4.03 mm), cm	0.0035		0.0028		0.0030	
L (Filter 2.41 mm), cm	0.0060		0.0023		0.0027	
L (Filter 1.75 mm), cm	0.0020		0.0012		0.0013	

- The appropriate operation of the triple-column system and the right use of the required gases allow the achievement of high performances with a limited consumption of gases.
- A theoretical approach considering that the culture growth was limited by four nutrients was developed and led to very accurate predictions of filter performance. The applicability and accuracy of the model was illustrated by comparing model predicted profiles with experimental data.
- The use of an inexpensive support media as gravel, as well as the use of solar-electrolysis hydrogen production system, makes the hydrogenotrophic denitrification economically viable for potable water treatment.

References

- [1] Council Directive 98/83/EC, L330/32, 5/12/1998, Official J. Eur. Communities, 1998.
- [2] B.T. Nolan, B.C. Ruddy, K.J. Hiitt and D.R. Helsel, A national look at nitrate contamination of ground water, *Water Cond. Purif.*, 39(12) (1998) 76–79.
- [3] V.J. Rijn, Y. Tal and H.J. Schreier, Denitrification in recirculating systems: Theory and applications, *Aquacul. Eng.*, 34(3) (2006) 364–376.
- [4] B.O. Mansell and E.D. Schroeder, Hydrogenotrophic denitrification in a microporous membrane bioreactor, *Wat. Res.*, 36(19) (2002) 4683–4690.
- [5] K.C. Lee and B.E. Rittmann, Applying a novel autohydrogenotrophic hollow-fiber membrane biofilm reactor for denitrification of drinking water, *Wat. Res.*, 36(8) (2002) 2040–2052.
- [6] S.J. Ergas and A.F. Reuss, Hydrogenotrophic denitrification of drinking water using a hollow fibre membrane bioreactor, *J. Wat. Supply: Res. Technol. – Aqua*, 50(3) (2001) 161–171.
- [7] H. Mo, J.A. Oleszkiewicz, N. Cicek and B. Rezanja, Hydrogen-dependent denitrification in an alternating anoxic–aerobic SBR membrane bioreactor, *Wat. Sci. Technol.*, 51(6–7) (2005) 357–364.
- [8] J.H. Shin, B.I. Sang, Y.C. Chung and Y.K. Choung, The removal of nitrogen using an autotrophic hybrid hollow-fiber membrane biofilm reactor, *Desalination*, 183 (2005) 447–454.
- [9] A. Terada, S. Kaku, S. Matsumoto and S. Tsuneda, Rapid autohydrogenotrophic denitrification by a membrane biofilm reactor equipped with a fibrous support around a gas-permeable membrane, *Biochem. Eng. J.*, 31(1) (2006) 84–91.
- [10] M.R. Schnobrich, B.P. Chaplin, M.J. Semmens and P.J. Novak, Stimulating hydrogenotrophic denitrification in simulated groundwater containing high dissolved oxygen and nitrate concentrations, *Wat. Res.*, 41(9) (2007) 1869–1876.
- [11] K.C. Lee and B.E. Rittmann, Effects of pH and precipitation on autohydrogenotrophic denitrification using the hollow-fiber membrane-biofilm reactor, *Wat. Res.*, 37(7) (2003) 1551–1556.
- [12] Y. Sakakibara and M. Kuroda, Electric prompting and control of denitrification, *Biotechnol. Bioeng.*, 42(4) (1993) 535–537.
- [13] Y. Sakakibara, T. Tanaka, K. Ihara, T. Watanabe and M. Kuroda, An in-situ denitrification of nitrate-contaminated groundwater using electrodes, *Proc. Environ. Eng. Res.*, 32 (1995) 407–415.
- [14] Z. Feleke, K. Araki, Y. Sakakibara, T. Watanabe and M. Kuroda, Selective reduction of nitrate to nitrogen gas in a biofilm-electrode reactor, *Wat. Res.*, 32(9) (1998) 2728–2734.
- [15] S. Islam and M.T. Suidan, Electrolytic denitrification: Long term performance and effect of current intensity, *Wat. Res.*, 32(2) (1998) 528–536.
- [16] Z. Feleke and Y. Sakakibara, A bio-electrochemical reactor coupled with adsorber for the removal of nitrate and inhibitory pesticide, *Wat. Res.*, 36(12) (2002) 3092–3102.
- [17] I.A. Vasiliadou, K.A. Karanasios, S. Pavlou and D.V. Vayenas, Experimental and modelling study of drinking water hydrogenotrophic denitrification in packed-bed reactors, *J. Hazard. Mater.*, 165 (2009) 812–824.
- [18] R. Grommen, M. Verhaege and W. Verstraete, Removal of nitrate in aquaria by means of electrochemically generated hydrogen gas as electron donor for biological denitrification, *Aquac. Eng.*, 34(1) (2006) 33–39.
- [19] C. Lu, P. Gu, P. He, G. Zhang and C. Song, Characteristics of hydrogenotrophic denitrification in a combined system of gas-permeable membrane and a biofilm reactor, *J. Hazard. Mater.*, 168 (2009) 1581–1589.
- [20] R. Vagheei, H. Ganjidoust, A.A. Azimi and B. Ayati, Nitrate removal from drinking water in a packed-bed bioreactor coupled by a methanol-based electrochemical gas generator, *Environ. Prog. Sust. Energ.*, 2009, doi: 10.1002/ep.10404.
- [21] Y. Sakakibara and T. Nakayama, A novel multi-electrode system for electrolytic and biological water treatments: electric charge transfer and application to denitrification, *Wat. Res.*, 35 (2001) 768–778.
- [22] M. Prosnansky, Y. Sakakibara and M. Kuroda, High-rate denitrification and SS rejection by biofilm-electrode reactor (BER) combined with microfiltration, *Wat. Res.*, 36(19) (2002) 4801–4810.
- [23] I.A. Vasiliadou, S. Pavlou and D.V. Vayenas, A kinetic study of hydrogenotrophic denitrification, *Process Biochem.*, 41(6) (2006) 1401–1408.
- [24] S. Ghafari, M. Hasan, M.K. Aroua, Effect of carbon dioxide and bicarbonate as inorganic carbon sources on growth and adaptation of autohydrogenotrophic denitrifying bacteria, *J. Hazard. Mater.*, 162 (2009) 1507–1513.
- [25] APHA, AWWA and WPCF, Standard Methods for the Examination of Water and Wastewater, 17th ed., American Public Health Association, 1989.
- [26] I. Shizas and D.M. Bagley, Measurement of dissolved hydrogen and hydrogen gas transfer in a hydrogen-producing reactor, *Anaerobic Digestion 10th World Congress*, Montreal, Quebec, Canada, Sept. 2004.
- [27] S. Ghafari, M. Hasan and M.K. Aroua, A kinetic study of autohydrogenotrophic denitrification at the optimum pH and sodium bicarbonate dose, *Bioresource Technol.*, 101(7) (2010) 2236–2242.
- [28] C.M. Ho, S.K. Tseng and Y.J. Chang, Autotrophic denitrification via a novel membrane-attached biofilm reactor, *Lett. Appl. Microbiol.*, 33(3) (2001) 201–205.
- [29] J.F. Andrews, A mathematical model for the continuous culture of microorganisms utilizing inhibitory substrates, *Biotechnol. Bioeng.*, 10(6) (1968) 707–723.
- [30] A. Tiemeyer, H. Link and D. Weuster-Botz, Kinetic studies on autohydrogenotrophic growth of *Ralstonia eutropha* with nitrate as terminal electron acceptor, *Appl. Microbiol. Biotechnol.*, 76(1) (2007) 75–81.
- [31] Y. Sakakibara, J.R.V. Flora, M.T. Suidan and M. Kuroda, Modeling of electrochemically-activated denitrifying biofilms, *Wat. Res.*, 28(5) (1994) 1077–1086.